



Efficient removal of chromium(VI) from dilute aqueous solutions using agro-industrial residue based on parboiled-rice husk ash

Vanessa Schwarstzhaupt Gamboa, Edilson Valmir Benvenuti, Éder Júlio Kinast, Marçal Pires, Fabiano Perin Gasparin & Lúcia Allebrandt da Silva Ries

To cite this article: Vanessa Schwarstzhaupt Gamboa, Edilson Valmir Benvenuti, Éder Júlio Kinast, Marçal Pires, Fabiano Perin Gasparin & Lúcia Allebrandt da Silva Ries (2021): Efficient removal of chromium(VI) from dilute aqueous solutions using agro-industrial residue based on parboiled-rice husk ash, Chemical Engineering Communications, DOI: [10.1080/00986445.2021.1948405](https://doi.org/10.1080/00986445.2021.1948405)

To link to this article: <https://doi.org/10.1080/00986445.2021.1948405>



Published online: 09 Jul 2021.



Submit your article to this journal [↗](#)



Article views: 31







View related articles [↗](#)



View Crossmark data [↗](#)



Efficient removal of chromium(VI) from dilute aqueous solutions using agro-industrial residue based on parboiled-rice husk ash

Vanessa Schwarztzaupt Gamboa^a , Edilson Valmir Benvenuti^b , Éder Júlio Kinast^a , Marçal Pires^c , Fabiano Perin Gasparin^b , and Lúcia Allebrandt da Silva Ries^a 

^aState University of Rio Grande do Sul, Porto Alegre, Rio Grande do Sul, Brazil; ^bFederal University of Rio Grande do Sul, Porto Alegre, Rio Grande do Sul, Brazil; ^cPontifical Catholic University of Rio Grande do Sul, Porto Alegre, Rio Grande do Sul, Brazil

ABSTRACT

The removal of Cr(VI) from wastewater by adsorption from agro-industrial residues remain an attractive option since combines reasonable cost with the quality of effluents treated. This paper employs of parboiled-rice husk ash (RHA) and parboiled-rice husk ash chemically treated (RHAH⁺) as adsorbents for Cr(VI). The RHA and RHAH⁺ were characterized. It was studied the adsorption efficiency on adsorbent dosage, pH, chromium concentration, and interaction time. RHAH⁺ presented superior Cr(VI) removal, although both adsorbents have shown satisfactory results. The best results are obtained at pH 1.0, presenting 90.9% and 97.7% of Cr(VI) removal for RHA and RHAH⁺, respectively, in 5 mg L⁻¹ of Cr(VI) concentration at about 30 minutes. The adsorption of RHAH⁺ is governed by the Freundlich isotherm ($R^2_{adj} = 0.989$) and kinetically by the pseudo-second order model ($R^2_{adj} = 0.991$). The rice husk ash represents an alternative low-cost and environment-friendly material that efficiently removes Cr(VI) from dilute aqueous solutions.

KEYWORDS

Adsorption; agro-industrial residue; Cr(VI); hexavalent chromium; parboiled-rice husk ash

1. Introduction

Contamination by heavy metals is a permanent environmental and health concern. Chromium is a transition metal that can exist in different oxidation states and is potentially harmful. In aqueous systems, the stable species Cr(III) and Cr(VI) are profuse (da Silva Ries and Silveira 2019), being Cr(VI) around 300 times more harmful than Cr(III), which makes it a risk for human health and the environment (Lin et al. 2018). Genotoxicity tests have shown that the hexavalent species causes mutagenic and carcinogenic effects on living organisms (Bielicka et al. 2005). In addition, it is bioaccumulative and non-biodegradable even at low concentrations (Burakov et al. 2018). Cr(VI) is typically associated with anthropogenic contamination from several industrial processes such as leather tanning, metallurgy and galvanization, chemical and petrochemical industries, textile dyeing, paint and pigment production, agricultural fertilizers, wood

preservatives, among others (Altun and Kar 2016; Lin et al. 2018). Particular care is required in handling and treating effluents containing Cr(VI) since it can easily flow into groundwaters and oceans, eventually compromising sources of drinking water. In effect, environmental agencies have established strict policies to comply with the concentration requirements of these species in wastewater. In Brazil, the maximum limits established for industrial wastewater discharge into water bodies are 0.1 mg L⁻¹ for Cr(VI) and 1.0 mg L⁻¹ for Cr(III) (CONAMA 2011).

In this sense, studies have been carried out to reduce wastewater generation and develop methods for removing these species in effluents, which include adsorption, ion exchange, chemical precipitation, ultrafiltration, electrochemical methods, reverse osmosis, bioremediation, membrane separation, among others (Aguiar et al. 2002; Burakov et al. 2018; Lin et al. 2018). However, each technique has its advantages and disadvantages and may in some cases be inefficient or

very costly (Dotto and McKay 2020) when applied to remove heavy metals in low concentrations. In that case, adsorption using commercial activated carbons is one of the most conventional technologies due to high efficiency, simplicity, and ease of operation. The adsorption process, at the same time, involves relatively high costs of the activated carbons as adsorbent. In recent years, the use of non-conventional adsorbents like lignocellulosic residues has arisen. These materials are typically available in large quantities from agro-industrial operations, and they represent a viable economic alternative of unexplored resources (Burakov et al. 2018).

Brazil is one of the largest rice producers in the world (approximately 12 million tons in 2019), with more than 25% corresponding to parboiled rice. The increasing incorporation of this grain in the diet is due to better nutritional properties compared to the white rice (Paraginski et al. 2014). In this manner, the increase in production leads to a rising amount of residue. Rice husk ash (RHA) is an abundant by-product obtained from the combustion of rice husk in parboiling and rice processing industries. RHA is chemically constituted by a mixture of oxides in which silica is the major compound, either in the amorphous or crystalline form. The rice husk represents around 20% of the total grain mass (Lopes and Lopes 2008). This percentage becomes significant considering the annual world production of about 770 million tons of rice in 2018, which corresponds to approximately 154 million tons of rice husk residues (Food and Agriculture Organization 2018). Currently, the disposal of large volumes of these solid residues has become a noticeable environmental problem to be managed. In particular, rice husk ash is a concern due to its fine structure and silica-rich chemical composition (average concentrations above 72–91% of SiO_2 , influenced by edaphoclimatic conditions) that makes its decomposition in the soil very slow (Salas et al. 1986; Della et al. 2006).

The increasing concern with the environment has headed several organizations and research institutions to seek technological alternatives that sustainably contribute to economic development. The application of residues as a raw material in

other processes can minimize the negative impacts on the environment. Using rice husk ash as adsorbent offers a potentially economic alternative for the removal of chromium from water (Foletto et al. 2005; Moayedi et al. 2019). Rice husk ash has been previously researched for the production of low-cost adsorbents, employing thermal and/or chemical treatments to modify the surface, increasing the selectivity and the adsorption capacity. Leaching processes using acids, bases, or organic solvents have been used to remove impurities. The surface and morphological aspects of the adsorbents have been modified through strong acids like hydrochloric, sulfuric, and phosphoric acids, the most used ones for this purpose (Wan Ngah and Hanafiah 2008; Fernandes et al. 2017).

Hexavalent chromium removal from aqueous solutions, especially at low concentrations, is a subject where innovations and cleaner and more economical methods are fundamental to deepen the current knowledge. The assessment of the parboiled-rice husk ash as adsorbent material can lead to cleaner technologies, linking the removal of one heavy metal from wastewater to an abundant and economic adsorbent. The interactions of the adsorbent and the contaminant must be evaluated to provide the basis for any potential technology of using parboiled-rice husk ash (RHA) as an efficient adsorbent for Cr(VI).

The present study aims to examine the feasibility of employing rice husk ash, an agro-industrial residue from the parboiling process, for removing hexavalent chromium from synthetic aqueous solution. A series of assessments were carried out, including the dependence of acid treatment on the adsorbent performance. Besides, the influence of experimental parameters like adsorbent dosage, pH, initial Cr(VI) concentration, and interaction time were studied. The isotherms models were fitted to investigate the adsorption capacity on the removal of chromium from dilute aqueous solution and the kinetic mechanism of the adsorption process was also assessed employing the parboiled-rice husk ash modified by sulfur acid (RHAH^+). Thus, two environmental problems can be solved simultaneously, the removal of chromium from effluents and the disposal of rice husk ash.

2. Material and methods

2.1. Materials and chemicals

The parboiled-rice husk ash (RHA) used in this work was provided by Cooperja Agroindustrial Cooperative, located in Brazil, in Santo Antonio da Patrulha city, state of Rio Grande do Sul. Deionized water and analytical grade reagents were used in the experiments.

2.2. Preparation of adsorbents

The parboiled-rice husk ash was milled and passed through a sieve (mesh 28) to ensure uniform particle size. Subsequently, the adsorbent was dried at 105 °C for 24 hours to achieve constant mass. This starting adsorbent material was named rice husk ash (RHA).

A fraction of the parboiled-rice husk ash was subjected to acid treatment using H₂SO₄ (1% v/v) to modify the surface characteristics. This treatment resulted in the adsorbent called rice husk ash chemically treated (RHAH⁺). The mixture of parboiled-rice husk ash and H₂SO₄ (solid-liquid ratio = 1:10) was kept in a laboratory autoclave at 121 °C and 1 atm for 60 minutes to prepare the RHAH⁺. Deionized water was used to wash the RHAH⁺ adsorbent until neutral pH, and later it was kept at 105 °C in the drying oven for 24 hours to achieve constant mass. Samples were stored into a desiccator for further experiments.

2.3. Adsorbents characterization

The surfaces of the prepared adsorbents described in Sec. 2.2 were subjected to morphological characterization by scanning electron microscopy (JEOL JSM 6060). All images were taken at 8 kV of accelerating voltage.

X-ray diffraction (XRD) was used to obtain the crystalline and non-crystalline nature of the materials. XRD patterns were obtained in a Siemens diffractometer D500, using Bragg-Brentano geometry. The equipment has Cu K α radiation (K α ₁ = 1.5406 Å and K α ₂ = 1.5444 Å), a curved graphite monochromator and it was calibrated with polycrystalline silicon. A scan step of 0.05° in 2 θ ranging from 8° to 100°, and a time interval of 1 second was used for the

measurements. Structure refinement was obtained by the program FullProf (Roisnel and Rodríguez-Carvajal 2001), and starting unit cell parameters were taken Wright and Leadbetter (1975).

The relative crystallinity was estimated according to Weidinger and Hermans (1961) with the ratio given by Eq. (1).

$$x_c = \frac{A_c}{A_c + A_a} \quad (1)$$

where A_c and A_a are the total crystalline and amorphous areas of the diffractogram. X-rays will be scattered in several directions in the amorphous phase, not showing high intensity narrow peaks, but a broad peak distributed over a wide range (2 θ).

Transmission infrared spectroscopy analysis was employed to identify the specific surface functional groups. FTIR was performed in a Nicolet 6700 FTIR spectrometer, using KBr as support. The spectral range varied from 4000 to 400 cm⁻¹ and the spectrum was obtained with 32 scans and 4 cm⁻¹ of resolution.

The specific surface area and pore size distribution were estimated based on nitrogen adsorption-desorption isotherms, obtained at 196 °C in a Micromeritics Tristar II Kr 3020 equipment. BET (Brunauer, Emmett and Teller) and the Horvath-Kawazoe methods were applied to estimate the surface area and the pore size distribution, respectively.

2.4. Adsorption experiments

2.4.1. Preparation of solutions

Potassium dichromate (K₂Cr₂O₇) was used as a base reagent for the preparation of synthetic Cr(VI) solutions, after drying at 105 °C to achieve constant mass, and stored into a desiccator for further use. The Cr(VI) stock solution (200 mg L⁻¹) was obtained by dissolving the salt into deionized water, while Cr(VI) concentration of the synthetic solutions changed from 5 to 100 mg L⁻¹, by diluting the stock solution. The pH of the Cr(VI) solutions was measured employing a pH meter (Digimed DM-31) before adsorption assays and the adjustment of pH was realized by 50% NaOH or 50% H₂SO₄ additions.

2.4.2. Batch adsorption assays

The assays were performed in batch mode employing both adsorbents (RHA and RHAH⁺) in 200 mL of synthetic solution. A conical flask of 250 mL was used to contain the solution and it was shaken at 25 °C and 180 rpm on a thermostatic shaker (Solab, SL-223). Under these conditions, it was investigated the effects on Cr(VI) adsorption with respect to the adsorbent dosage (5 and 15 g L⁻¹), pH solution (pH 1.0, 3.0, 5.0 and 7.0), initial Cr(VI) concentration (5, 20 and 45 mg L⁻¹) and interaction time (0.25, 0.50, 1, 2, 3, 4 and 24 hours).

Each experiment was executed in duplicate and the mean value was considered for data analysis. After the adsorption interaction time, the mixture was centrifuged for 15 minutes at 3000 rpm (Nova Técnica NT 810). The supernatant was collected, and then the residual Cr(VI) concentration was quantified via colorimetric analysis according to the standard APHA method (American Public Health Association 1995) with a UV-Vis spectrophotometer (Perkin-Elmer Lambda—265 UV/Vis). Absorbance was measured at a wavelength of 540 nm. Cr(VI) reacts with 1,5-diphenylcarbazide in acid solution, producing a purple colored complex.

The adsorption efficiency of both adsorbents (RHA and RHAH⁺) was calculated by Eq. (2):

$$\text{Adsorption efficiency (\%)} = \frac{C_0 - C_f}{C_0} \cdot 100 \quad (2)$$

where C_0 (mg L⁻¹) is the initial concentration and C_f (mg L⁻¹) is the final concentration of Cr(VI).

2.5. Adsorption isotherms study

The ability of an adsorbent to accumulate on its surface a certain amount of the adsorbate under equilibrium conditions is estimated by adsorption isotherms. They can provide significant information on the surface properties and affinity of the adsorbent to reach its highest adsorption capacity. Adsorption isotherms can be expressed graphically or by equations that relate the amount of the adsorbed species, such as heavy metals on a solid adsorbent, at a given temperature (Attari et al. 2017).

The equilibrium data obtained from Cr(VI) adsorption on RHA and RHAH⁺ were analyzed employing Langmuir and Freundlich models, the most used ones to describe experimental data.

The experiments for the evaluation of the adsorption isotherms were conducted using solutions with 5, 20, 45, 52.5, 60, 72.5, 85, and 100 mg L⁻¹ with 5 g L⁻¹ of adsorbent in pH 1.0 and 24 hours of interaction time. The adsorption capacity of Cr(VI) is given by Eq. (3).

$$q_e = \frac{(C_0 - C_e) \cdot V}{m} \quad (3)$$

where q_e (mg g⁻¹) is the amount of adsorbed solute per gram of adsorbent, C_0 (mg L⁻¹) is the initial Cr(VI) concentration, C_e (mg L⁻¹) is the Cr(VI) concentration at the equilibrium, V (L) is the volume of Cr(VI) solution used and m (g) is the mass of the adsorbent applied.

2.5.1. Langmuir isotherm model

The adsorption process was assessed via the Langmuir isotherm, given by Eq. (4). This model assumes that there is a definite number of sites with equivalent energy and the molecules do not interact with each other. It also assumes that adsorption takes place on a monolayer and uniform surface and that each site contains only one adsorbed molecule (Nascimento et al. 2014).

$$q = \frac{q_{\max} \cdot K_L \cdot C_e}{1 + K_L \cdot C_e} \quad (4)$$

where q (mg g⁻¹) represents the amount of adsorbed solute per gram of adsorbent, q_{\max} (mg g⁻¹) the maximum adsorption capacity, K_L (L mg⁻¹) the adsorbent–adsorbate interaction constant and C_e (mg L⁻¹) is the equilibrium adsorbate concentration.

The separation coefficient (R_L) is a dimensionless parameter of the Langmuir isotherm defined by Eq. (5) (Khandaker et al. 2017):

$$R_L = \frac{1}{1 + K_L \cdot C_0} \quad (5)$$

where C_0 (mg L⁻¹) is the initial Cr(VI) concentration and K_L (L mg⁻¹) the adsorbent–adsorbate interaction constant. The favoring of the adsorption process is indicated by R_L value in unfavorable ($R_L > 1$), linear ($R = 1$), favorable ($0 < R_L < 1$) and irreversible ($R_L = 0$).

Another parameter related to the Langmuir isotherm relevant to interpret the adsorption process is the surface covered fraction (Θ), expressed by Eq. (6).

$$\theta = \frac{K_L \cdot C_0}{1 + K_L \cdot C_0} \quad (6)$$

where K_L (L mg^{-1}) is the Langmuir constant, C_0 (mg L^{-1}) is the initial Cr(VI) concentration and Θ is the surface coverage.

2.5.2. Freundlich isotherm model

The amount of adsorbed solute and the concentration of the solute in the solution are related through the Freundlich isotherm, an empirical model that can be employed to multilayer adsorption, and non-ideal systems. This model considers that the adsorbent surface (solid phase) is heterogeneous and the adsorption sites present different energy distributions. That is, it is assumed that the sites are distributed logarithmically, therefore, the solute (adsorbate) binding to the solid phase surface occurs more strongly in some sites than in others (Nascimento et al. 2014). Freundlich's isotherm is described by Eq. (7).

$$q_e = K_f \cdot C_e^{1/n} \quad (7)$$

where q_e (mg g^{-1}) is the amount of adsorbed solute per gram of adsorbent, C_e (mg L^{-1}) is the equilibrium concentration of the solute, $1/n$ is the surface heterogeneity constant referring to adsorption intensity, and K_f ($\text{mg}^{1-(1/n)} \text{g}^{-1} \text{L}^{1/n}$) is the Freundlich constant concerning the adsorption capacity.

2.6. Kinetic study

In order to assess the adsorption process mechanism a series of essays were developed using the best conditions defined in the previous steps, such as pH 1, amount of adsorbent of 5 g L^{-1} and amount of adsorbate of 45 mg L^{-1} . The temperature evaluated was 25°C . Samples were collected at 0.25, 0.50, 1, 2, 3, 4 and 24 hours. Kinetic mechanisms of pseudo-first order and pseudo-second order were used to evaluate the results obtained.

2.6.1. Pseudo-first order

The model of pseudo-first order is given by Eq. (8) (Nascimento et al. 2014; Martini et al. 2020):

$$\frac{\partial q_t}{\partial t} = k_1(q_e - q_t) \quad (8)$$

where k_1 is the pseudo-first order adsorption rate constant (min^{-1}), q_e and q_t (mg g^{-1}) are the amount of ions adsorbed per gram of adsorbent at equilibrium and at time t , respectively, and t is the interaction time between adsorbent and adsorbate. To find the value of k_1 , it was used the linearized equation (Eq. (9)) and the plot of $\ln(q_e - q_t)$ versus t .

$$\ln(q_e - q_t) = \ln q_e - k_1 t \quad (9)$$

2.6.2. Pseudo-second order

The pseudo-second order model is expressed by Eq. (10) (Nascimento et al. 2014; Martini et al. 2020).

$$\frac{\partial q_t}{\partial t} = k_2(q_e - q_t)^2 \quad (10)$$

where k_2 is the pseudo-second order adsorption rate constant ($\text{g mg}^{-1} \text{min}^{-1}$), q_e and q_t are the amount (mg g^{-1}) of ions adsorbed at equilibrium and at time t , respectively. The linear form of Eq. (10) is shown below (Eq. (11)) and a linear fit of t/q_t versus t gives k_2 value.

$$\frac{t}{q_t} = \frac{1}{k_2 q_e^2} + \frac{t}{q_e} \quad (11)$$

3. Results and discussion

In this section, the results of the characterization and adsorption assays of RHA and RHAH⁺ adsorbents are presented and discussed.

3.1. Adsorbent characterization

3.1.1. Scanning electron microscopy (SEM)

The SEM allows the visualization of the surface microstructures of the materials. The SEM images for both adsorbents are exhibited in Figure 1. The surface of RHA (Figure 1A) is rugged with irregular cavities of various dimensions that can indicate the presence of partially burned materials. The surface roughness is attributed to the oxidation and/or evaporation of organic

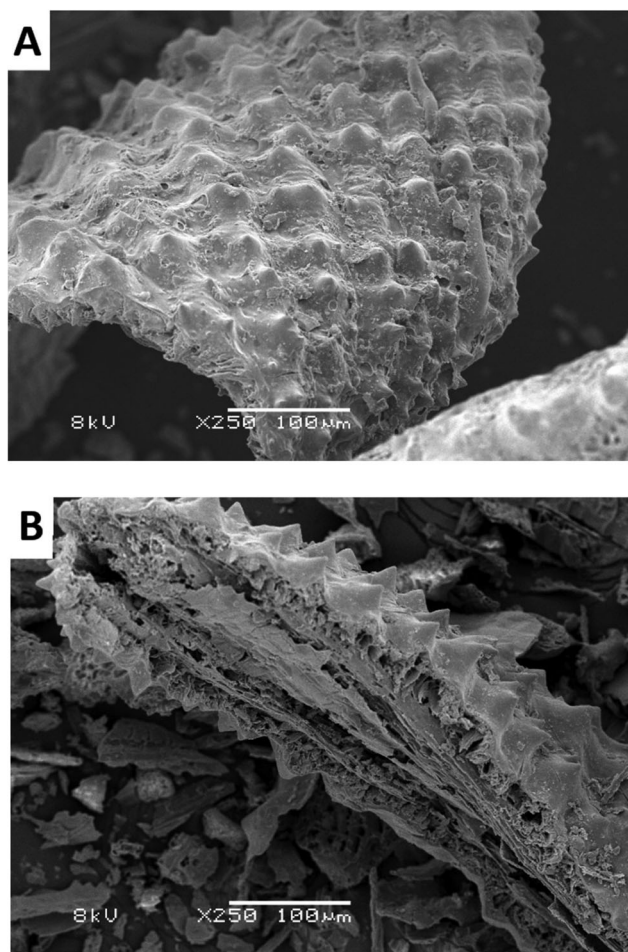


Figure 1. SEM images (A: RHA and B: RHAH⁺).

compounds that were converted into gases during the combustion process. A similar observation concerning the presence of rough surfaces was also observed by Mor et al. (2016) when studying rice husk ash for the removal of phosphate from the wastewater. In contrast, this material when chemically treated (RHAH⁺) acquires a highly heterogeneous surface, with a series of cavities and channels of varying sizes and fine pores arranged randomly throughout the material structure (Figure 1B). In general, materials resulting from acid treatment present greater irregularity and a larger number of cavities on their surfaces. The increase in heterogeneity is assigned to matrix deterioration after thermal and chemical treatments, due to the partial decomposition of cellulose, hemicelluloses, and lignin. The large number of cavities, channels, and surface disorder found in RHAH⁺ is closely linked to the efficiency of the adsorption process. Micropores are formed, expanding the internal surface area and

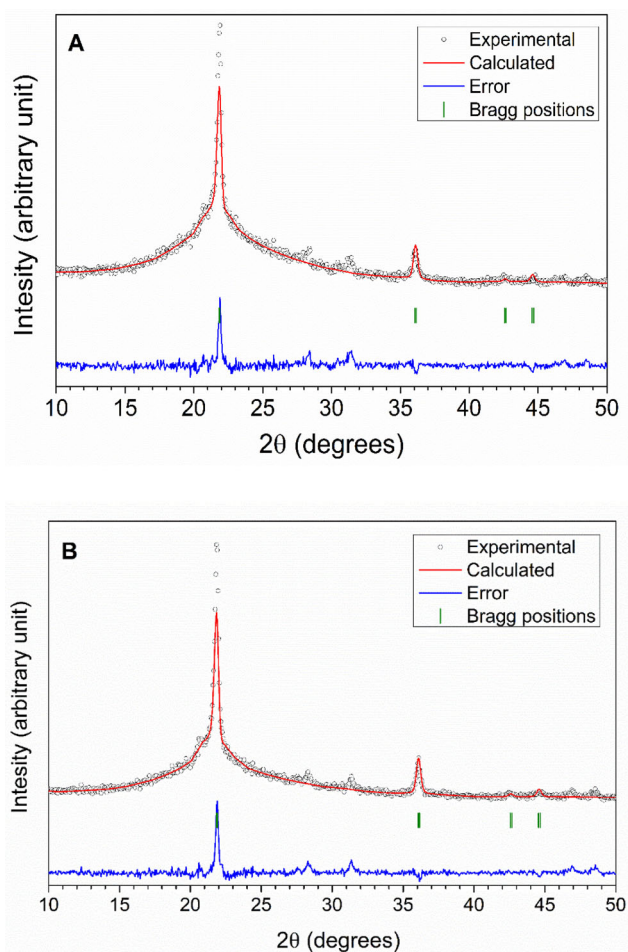


Figure 2. The relevant part of the X-ray powder diffraction pattern for (A) RHA and (B) RHAH⁺ adsorbents. Observed data are depicted by open circles. Rietveld refinement (calculated pattern) is given by the red solid line. Green bars indicate Bragg reflections. Residual intensity is plotted as the blue line.

enhancing the accessibility of reactive centers on the adsorbents. During the adsorption assays carried out under agitation, it is assumed that cavities and channels serve as access to the micropores where interaction with the active sites and adsorption can occur.

3.1.2. X-ray diffraction (XRD)

The X-ray diffractograms (Figure 2) reveal Bragg reflections (2θ) in 22.5° and 36.5° for both adsorbents, characteristic of lignocellulosic materials (El Halal et al. 2015). The crystallinity is $6\% \pm 2\%$ for RHA and $9\% \pm 2\%$ for RHAH⁺, thus, both adsorbents are mostly amorphous.

The Rietveld refinements demonstrate the presence of SiO₂ with a cubic crystalline

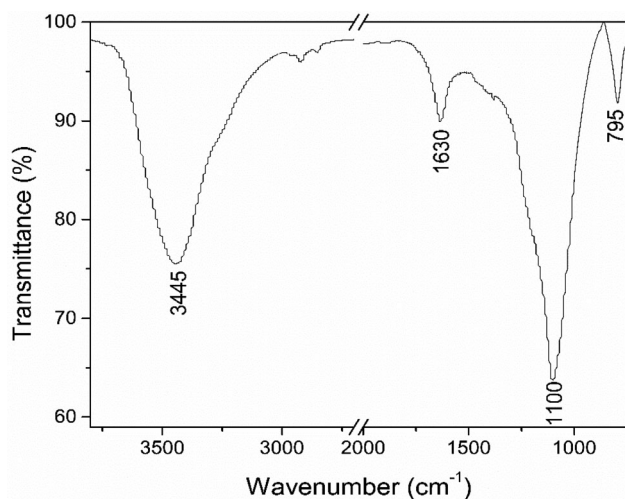


Figure 3. Transmission infrared spectrum for RHA adsorbent.

structure, called β -cristobalite, with $Fm\bar{3}d$ space group. The cell lattice parameters are $a = 7.03(1)$ Å and $a = 7.03(4)$ Å for RHA and RHAH⁺, respectively. The standard deviation of the measurement is given by the numbers in parentheses on the last decimal presented. The analyzes do not show relevant Bragg reflections beyond 50 degrees.

Crystallinity is favored by the increase in combustion temperature and residence time of the adsorbents. The degree of crystallinity also influences the adsorption process, where predominantly amorphous structures are the most used for this process due to higher heterogeneity in their structure (Xiong et al. 2009).

3.1.3. Fourier transform infrared spectroscopy (FTIR)

Figure 3 shows the infrared analysis of RHA material, before the adsorption assay. The spectrum shows a typical silica profile, with Si-O bond, and stretching modes at 795 and 1100 cm^{-1} (Costa et al. 1997; Fidalgo and Ilharco 2001). The band with a maximum around 3445 cm^{-1} is interpreted as a consequence of the superposition of hydroxyl stretching bands of silanol groups and adsorbed water. The band at 1636 cm^{-1} is by virtue of the bonding of physically adsorbed water (Costa et al. 1997). Therefore, the infrared spectrum reveals that the RHA material is predominantly silica, with an appreciable amount of silanol on the surface since water is adsorbed thereon. The silanol groups, when acid-activated, play an important role as

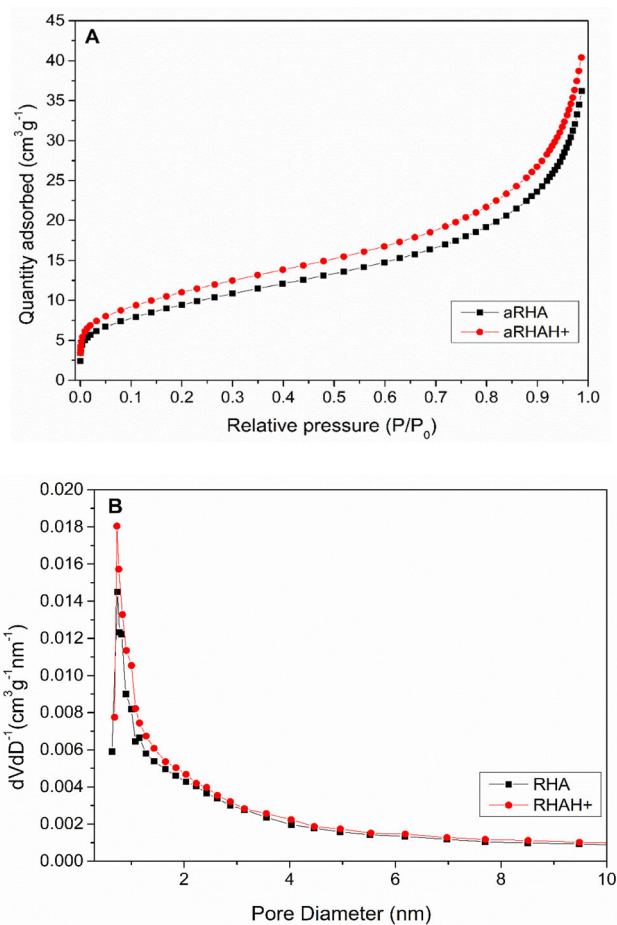


Figure 4. Textural analysis: (A) Nitrogen adsorption isotherms (B) Horwath-Kawazoe pore size distribution.

adsorbent (Ahmaruzzaman and Gupta 2011; Singh and Singh 2012; Ghosh 2013; Mor et al. 2016). Similar behavior was obtained for the RHAH⁺ (not shown).

3.1.4. Bet surface area analysis

The most significant characteristics regarding the adsorption capacity of materials are the surface area and porosity (Song et al. 2018). Aiming to clarify and quantify the surface of the ash, a textural analysis was performed, before and after the acid treatment. The nitrogen adsorption isotherms are shown in Figure 4(A). The isotherms present type II profile, typical of non-porous materials. However, they present slight inflections at low relative pressures ($P/P_0 < 0.1$) that demonstrate a fraction of micropores, with a diameter lower than 2 nm (Gregg and Sing 1982). The estimated BET surface area values were 34 and 39 ± 2 $\text{m}^2 \text{g}^{-1}$ for RHA and RHAH⁺, respectively. The Horwath-Kavazoe pore size distribution

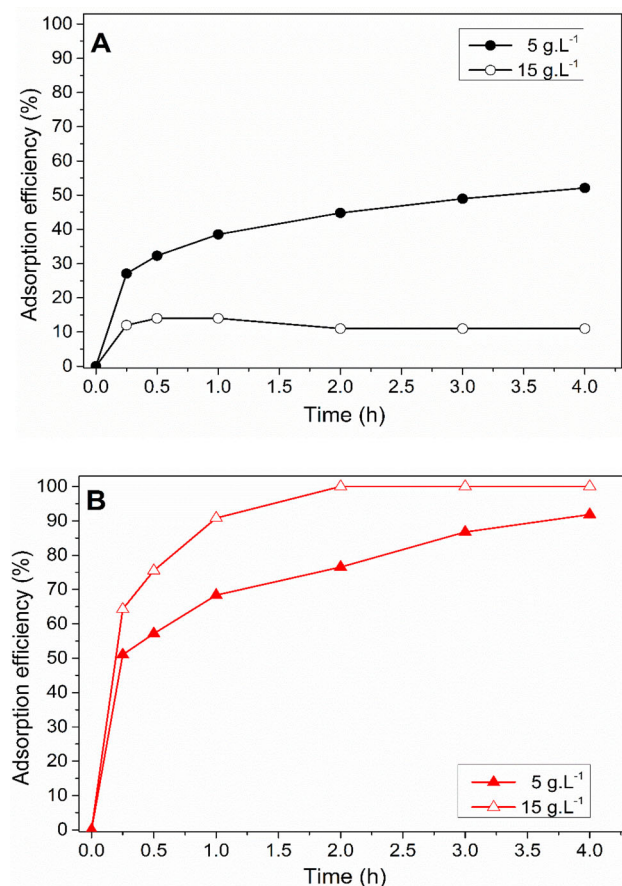


Figure 5. Chromium(VI) removal efficiency using parboiled-rice husk ash (A: RHA and B: RHAH⁺) at different adsorbent dosages. Conditions: 5 mg L⁻¹ of Cr(VI); 25 °C; pH 3.0; 180 rpm.

curves are shown in Figure 4(B), confirming the microporosity of the adsorbents studied.

3.2. Adsorption experiments

3.2.1. Effect of adsorbent dosage

Adsorbent dosage on the removal of Cr(VI) in aqueous solution was investigated by experiments using 200 mL of Cr(VI) solution at an initial concentration of 5 mg L⁻¹. Two dosages of adsorbents were added (5 g L⁻¹ and 15 g L⁻¹), at 25 °C, pH 3.0, agitation speed of 180 rpm, and interaction times up to 4 hours.

Figure 5(A) and 5(B) shows the removal efficiency of Cr(IV) over time for the two dosages of both adsorbents (RHA and RHAH⁺). The adsorbent chemically treated, for the dosage of 15 g L⁻¹, presents a significant efficiency compared to the dosage of 5 g L⁻¹ (Figure 5B). This is because since the higher adsorbent dosage the higher specific surface area available for

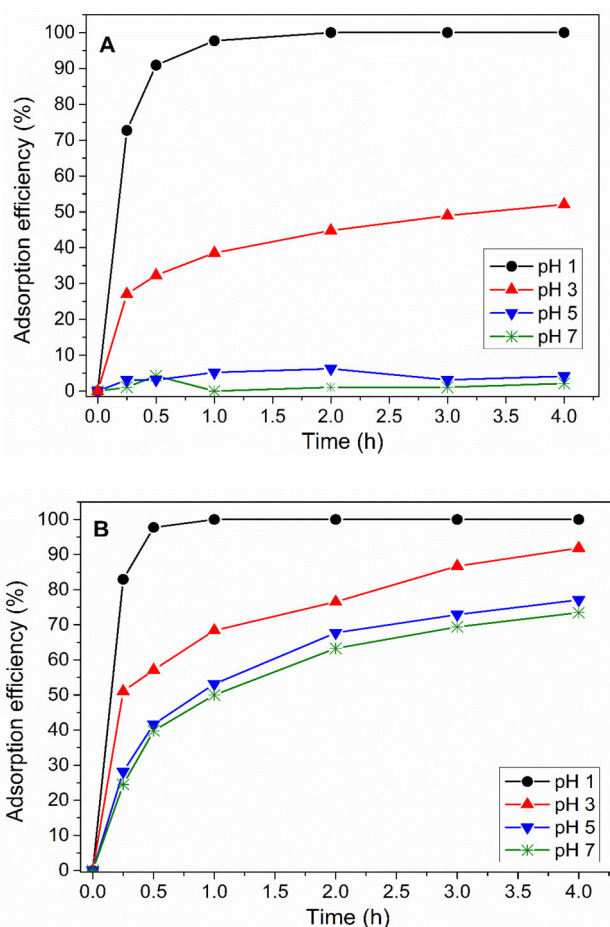


Figure 6. Chromium(VI) removal efficiency using parboiled-rice husk ash (A: RHA and B: RHAH⁺) at different pH values. Conditions: 5 mg L⁻¹ of Cr(VI); 5 g L⁻¹ of adsorbent dosage; 25 °C; 180 rpm.

adsorption, resulting in larger interaction between adsorbent and adsorbate. Similar results were reported by Altun and Kar (2016), Babel and Kurniawan (2004), and Enniya et al. (2018), who investigated the removal of hexavalent chromium in aqueous solution on adsorbent materials prepared from various biomasses. Figure 5(B) reveals that RHAH⁺ presents 100% of efficiency, for the dosage of 15 g L⁻¹, and 76.2% for the dosage of 5 g L⁻¹, after 2 hours of interaction.

The values of chromium removal efficiency for both adsorbents are quite different mainly due to the effects of surface modification by acid treatment. It was not evidenced for RHA the same potentiating effect of the higher adsorbent dosage on the chromium removal. This finding may be related to the obstruction of active sites by solid particle conglomerates, which make it difficult for chromium species to interact on the surface

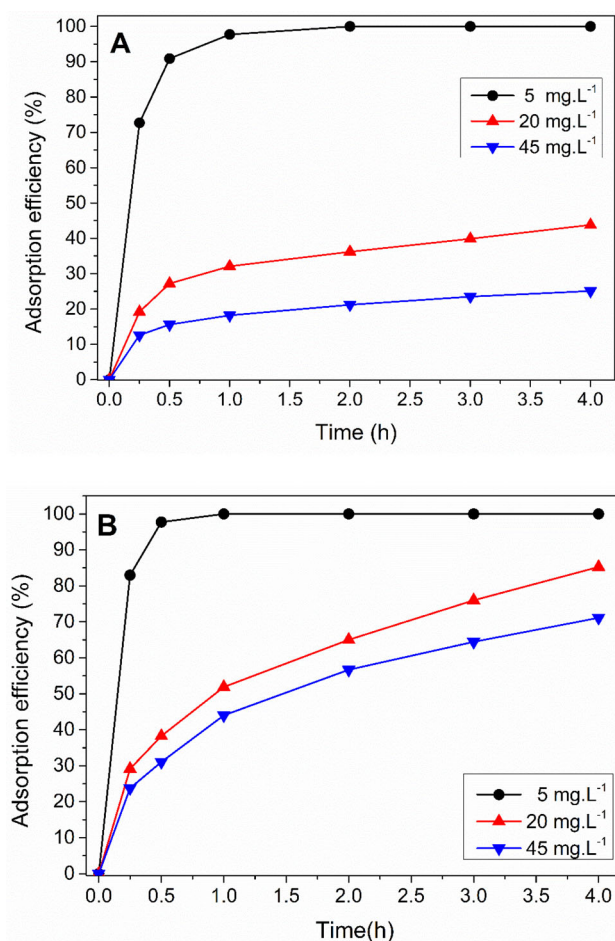


Figure 7. Chromium(VI) removal efficiency using parboiled-rice husk ash (A: RHA and B: RHAH⁺) at different Cr(VI) concentrations. Conditions: 5 g L⁻¹ of adsorbent dosage; pH 1.0; 25 °C; 180 rpm.

of the adsorbent (Kannan and Sundaram 2001; Raposo et al. 2009). A similar result was obtained by Wu et al. (2017) who worked on the adsorption of chromium onto bamboo charcoal.

Due to the effect observed with the RHA, the subsequent experiments were defined using 5 g L⁻¹ of adsorbent in each assay.

3.2.2. Effect of pH

The dependence of the adsorption process on the pH is explained by the adsorbent surface charge and the speciation of the adsorbate in the solution. The effect of pH on the Cr(VI) removal by RHA and RHAH⁺ adsorbents was conducted at pH values ranging from 1.0 to 7.0. The experiments were performed with 200 mL of Cr(VI) solution at a concentration of 5 mg L⁻¹, adsorbent dosage of 5 g L⁻¹, at 25 °C, agitation speed of 180 rpm, and interaction times up to 4 hours.

The results depicted in Figure 6(A) and 6(B) show that the removal efficiencies of both adsorbents clearly amplified while pH varied from 7.0 to 1.0. At pH 1.0 and about 30 minutes of interaction time, the Cr(VI) adsorption efficiency is 90.9% for RHA, and 97.7% for RHAH⁺. At pH 5.0 and 7.0, only the RHAH⁺ showed significant removal values, 77.1% and 73.5% respectively, in about 4 hours. RHAH⁺ always presents higher adsorption percentages compared to RHA, indicating the superior performance of the adsorbent chemically treated with H₂SO₄.

As described previously (Ahmed et al. 2012; Altun and Kar 2016; Kieling et al. 2019; Mitra et al. 2019; da Silva Ries and Silveira 2019), the lower the pH of the solution the higher the chromium removal. This trend is explained by a highly protonated adsorbent surface obtained in strong acidic conditions, which leads to a high adsorption of anionic Cr(VI), because of the strong electrostatic attraction constituted (Bielicka et al. 2005). The stability of Cr(VI) anionic forms depends on the pH of the solution (Hamadi et al. 2001; Zhao et al. 2005; Liu et al. 2007). At pH 1.0, the chromium exist as H₂CrO₄, however in the pH range from 1.0 to 5.0 different forms of chromium ions coexist, of which HCrO₄⁻ remains the predominant one (Srivastava et al. 2013; Zeljkovic et al. 2015; Enniya et al. 2018). This interpretation explains the high Cr(VI) adsorption efficiency at an acid solution. As pH increases, HCrO₄⁻ is replaced by CrO₄²⁻ and Cr₂O₇²⁻ ions (Zhao et al. 2005). The protonation intensity of the material surface (RHA and RHAH⁺) decreases while the concentration OH⁻ ions increases, which leads to the reduction of electrostatic attraction between negatively charged chromium ions and the adsorbent surface. The result of this charge balance is a depletion in the chromium removal efficiency as the pH of the solution increases. Due to better adsorption results at pH 1.0, the subsequent experiments were conducted at this pH value.

3.2.3. Effect of initial chromium concentration

The removal of Cr(VI) ion by RHA and RHAH⁺ adsorbents was assessed through adsorption assays employing initial concentrations of 5, 20, and 45 mg L⁻¹ on each adsorbent. The

experiments were performed using 200 mL of Cr(VI) solution, an adsorbent dosage of 5 g L^{-1} , pH 1.0, at 25°C , agitation speed of 180 rpm, and interaction times up to 4 hours. Figure 7(A) and 7(B) presents the effect of the initial Cr(VI) concentration on the adsorption efficiency as a function of the interaction time.

With the increment of the initial concentration of Cr(VI), the adsorption capacity (mg g^{-1}), given by Eq. (3), also increases for the two adsorbents. After a interaction time of 1 hour, the adsorption capacities are 0.9772, 1.284 and 1.638 mg g^{-1} for RHA and 1.000, 2.075 and 3.960 mg g^{-1} for RHAH⁺ for initial concentrations of 5, 20 and 45 mg L^{-1} , respectively. The observed improvement in the adsorption capacity of chromium with its concentration in the solution is probably a consequence of the augmentation in the driving force of the concentration gradient (Enniya et al. 2018).

Figure 7(A) and 7(B) shows that chromium adsorption increases over time, initially at a high rate, and then tends to reach equilibrium. At low concentrations, the ratio of active sites is larger, so the removal occurs at a higher rate. However, when the concentration increases, the ratio of sites is lower, showing noticeable reduction in chromium removal efficiency. Similar results were reported previously for charcoals prepared from different sources of biomass (Karthikeyan et al. 2005; Altun and Kar 2016; Enniya et al. 2018).

The RHAH⁺ showed higher removal efficiency than RHA, for the three concentrations studied, probably because of the higher availability of active sites generated by acid treatment. Efficiency of 100% is achieved at the concentration of 5 mg L^{-1} in 2 hours for RHA and in 1 hour for RHAH⁺.

3.2.4. Effect of interaction time

Interaction time is a relevant parameter regarding the removal of a pollutant. The interaction time effect on the removal of Cr(VI) by both adsorbents was assessed through a series of adsorption experiments employing concentrations of 20 and 45 mg L^{-1} on each adsorbent. The concentration of 5 mg L^{-1} was not explored because it already

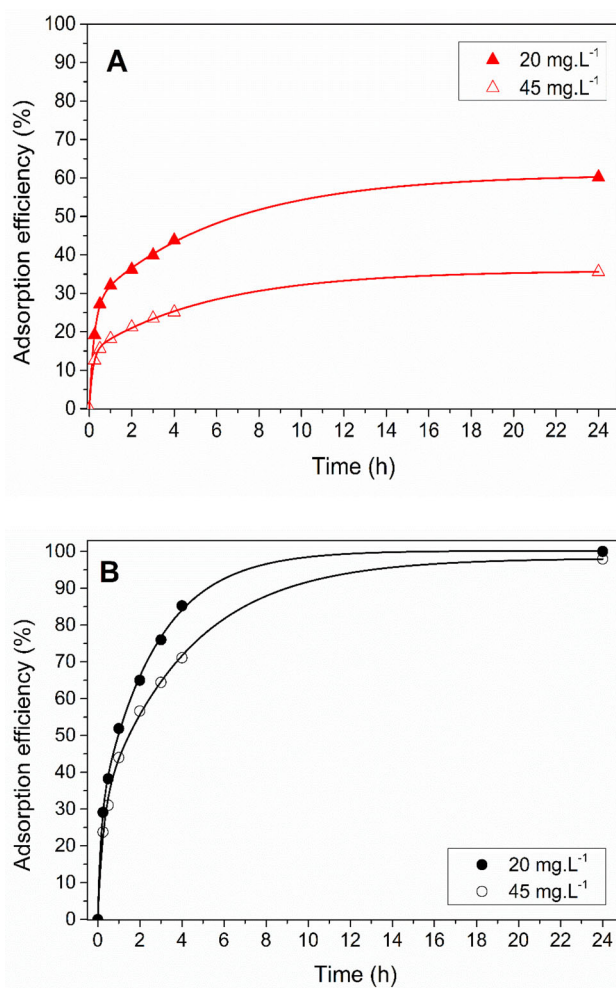


Figure 8. Estimation of interaction time to reach adsorption equilibrium at 20 mg L^{-1} and 45 mg L^{-1} of Cr(VI). (A: RHA and B: RHAH⁺). Conditions: 5 g L^{-1} of adsorbent dosage; pH 1.0; 25°C ; 180 rpm.

reached 100% efficiency removal in about 1–2 hours of interaction time (Figure 7).

Data were collected at interaction times of 0.25, 0.50, 1, 2, 3, 4, and 24 hours. The latter time is not viable for industrial plants, it was included just to perform mathematical modeling.

The experiments were performed using 200 mL of Cr(VI) solution, adsorbent dosage of 5 g L^{-1} , pH 1.0, at 25°C , agitation speed of 180 rpm, and interaction times up to 24 hours. The effect of the interaction time is shown in Figure 8(A) and 8(B) for both adsorbents. Chromium removal increased with interaction time as expected. At the beginning of the process, high adsorption rates were recognized, because of the abundance of sites favorable to adsorbent-adsorbate interactions. The surface is quickly saturated with chromium ions during the early stage of adsorption.

Table 1. Langmuir and Freundlich isotherms parameters for the adsorption of chromium on RHAH⁺ adsorbent.

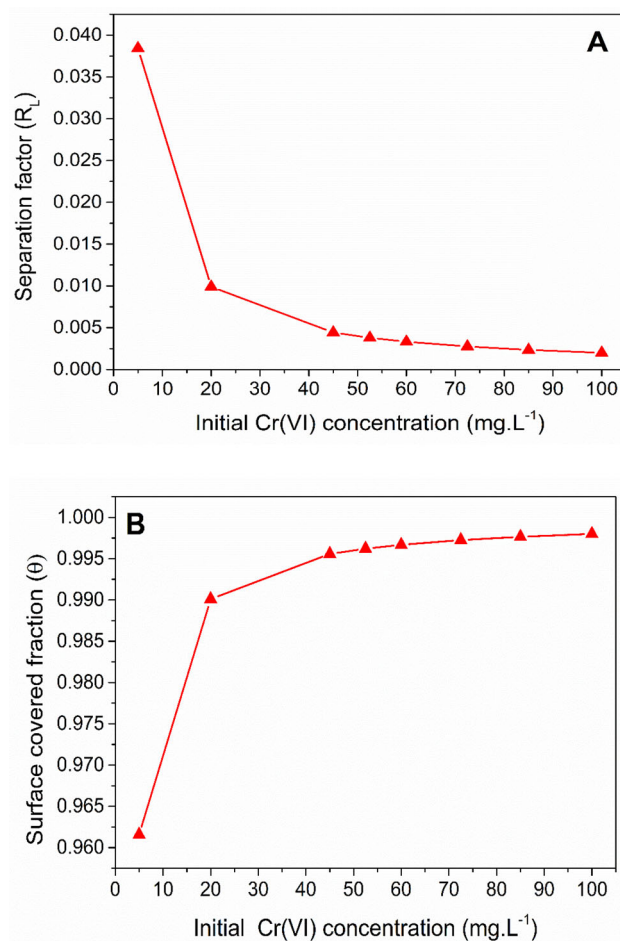
Equations	Parameters	RHAH ⁺	R ² _{adj}
Langmuir	q _{max}	27.354 mg g ⁻¹	0.951
	K _L	5.004 L mg ⁻¹	
Freundlich	K _f	27.896 mg ^{1-(1/n)} g ⁻¹ L ^{1/n}	0.989
	n	2.167	

In the later stages, the rate of adsorption decreases as ions diffuse into the micropores, resulting in greater resistance due to higher steric hindrance, and thus requiring long interaction times (Altun and Kar 2016). The adsorption efficiency for the RHA, in 24 hours, was 60.2% and 35.6% for 20 and 45 mg L⁻¹, respectively. Whereas RHAH⁺ showed 100% and 98.1% for 20 and 45 mg L⁻¹, respectively. A mathematic function was adjusted to the experimental data to evaluate the adsorption process. Both adsorbents, RHA and RHAH⁺, reach the equilibrium before 24 hours. Figure 8(A) shows that RHA reach equilibrium at 22.2 hours (60.0% removal efficiency) for 20 mg L⁻¹ and at 18.2 hours (35.0% removal efficiency) for 45 mg L⁻¹. The enhanced performance of the adsorbent chemically treated was verified. RHAH⁺ exhibited equilibrium at 15.9 hours (100% removal efficiency) and at 17.2 hours (97.0% removal efficiency) for 20 and 45 mg L⁻¹, respectively.

3.2.5. Adsorption isotherms

Adsorption isotherms were plotted in a wide range of chromium concentrations (from 5 to 100 mg L⁻¹), for RHAH⁺, an adsorbent dosage of 5 g L⁻¹, pH 1.0, agitation speed of 180 rpm, and 24 hours of interaction time. The equilibrium data were analyzed via Langmuir and Freundlich isotherms models. Table 1 presents the results found for both adsorption isotherms.

The Freundlich isotherm fits more appropriately to the experimental data (R²_{adj} = 0.989) than the Langmuir isotherm (R²_{adj} = 0.951). The maximum calculated Freundlich isotherm adsorption capacity (K_F) is 27.896 mg^{1-(1/n)} g⁻¹ L^{1/n}. Nevertheless, both isotherms can be used to explain the adsorption mechanism. There is a trend in the literature to adjust the adsorption behavior of rice husk ash to the Freundlich isotherm for different adsorbates (Ahmed et al. 2012; Rahaman et al. 2015). This trend may be

**Figure 9.** The separation factor, R_L , (A) and the surface coverage, Θ , (B) parameters against the initial concentration on Cr(VI) adsorption for RHAH⁺ adsorbent.

associated with the high surface heterogeneity of this adsorbent, a consequence of thermal and chemical treatments, as evidenced by the scanning electron microscopy (Figure 1).

Values for the separation factor (R_L) can be obtained with the Langmuir isotherm. For the entire range of chromium concentration studied (from 5 to 100 ppm) the R_L values found were between 1 and 0 ($0 < R_L < 1$), according to Figure 9(A), demonstrating the favorability of the chromium adsorption process by RHAH⁺. The chromium adsorption process can also be evaluated using the surface coverage (Θ) parameter. The coverage factor was plotted as a function of the initial Cr(VI) concentration in Figure 9(B). Initially, a large increase occurs with the increase in concentration, and then a gradual decrease at the rate is observed, with the theta value (Θ) tending to 1 from 20 mg. L⁻¹ of the chromium

Table 2. Adsorption isotherms and parameters for the removal of chromium by RHAH⁺ and other adsorbents found in the literature.

Adsorbent	Langmuir isotherm (q_{\max})	Freundlich isotherm (K_f)	Reference
Parboiled-rice husk ash chemically treated (RHAH ⁺)	27.35	27.90	This research
Rice husk ash	1.70	1.43	(Kieling et al. 2019)
Rice husk	11.40	2.98	(Mitra et al. 2019)
Calcined rice husk	0.085	13.04	(Srivastava et al. 2013)
carbonized pineapple leaves	18.77	0.06	(Ponou et al. 2011)
Coconut shell	18.70	3.46	(Singha and Das 2011)
Magnetic biochar of sugarcane bagasse	43.12	21.29	(Yi et al. 2019)
Magnetic biochar of rice straw	33.23	20.82	(Yi et al. 2019)
Treated waste newspaper	36.32	11.84	(Dehghani et al. 2016)
Sugar cane bagasse	13.23	0.26	(Sharma and Forster 1994)
Sawdust	1.93	–	(Hamadi et al. 2001)
<i>Hevea Brasiliensis</i> sawdust activated carbon	44.05	25.48	(Karthikeyan et al. 2005)

concentration. These results have shown that RHAH⁺ is an efficient adsorbent to remove Cr(VI) from the dilute aqueous solution.

Table 2 presents a comparison of previous studies about Cr(VI) removal with the present work. The data illustrate the adsorption capacity presented by the parboiled-rice husk ash chemically treated, demonstrating the ability of this material to act as a promising adsorbent of chromium ions in wastewaters.

3.2.6. Kinetic analysis

The two kinetic models applied showed good correlation for the generated results. Among them, the pseudo-second order presented a better fit and a higher R^2_{adj} , demonstrating that the data are more appropriately adjusted to this kinetic model. The pseudo-first order and pseudo-second order constants and the corresponding correlation values are shown in Table 3.

According to Ho and McKay (2000), the pseudo-second order kinetic model describes the processes that involve a chemisorption. Based on the pseudo-second order kinetic model assumptions the reaction rate is proportional to the number of active sites on the adsorbent surface and the chemical adsorption can be the step rate-limiting of the process (Agrafioti et al. 2014). This result is in agreement with other works reported in literature for Cr(VI) removal by different biosorbents (Georgieva et al. 2015; Ding et al. 2016; Singh et al. 2021).

4. Conclusions

The cost-effective adsorbents from the ash of the parboiled-rice husk (RHA and RHAH⁺), for

Table 3. Parameters of kinetic modeling for Cr(VI) adsorption by RHAH⁺.

Pseudo-first order		Pseudo-second order	
K_1 (min^{-1})	R^2_{adj}	K_2 ($\text{g mg}^{-1} \text{min}^{-1}$)	R^2_{adj}
–0.266	0.979	0.165	0.991

removing chromium(VI) from dilute aqueous solutions were assessed. The parboiled-rice husk ash (RHA) and parboiled-rice husk ash chemically treated (RHAH⁺) were used as adsorbent materials, the latter exhibiting higher removal potential. The morphological, chemical and structural characterizations performed via scanning electron microscopy (SEM), X-ray diffraction (XRD), Fourier transform infrared spectroscopy (FTIR), and BET (Brunauer, Emmett and Teller) surface area analysis showed that RHAH⁺ adsorbent has a considerable heterogeneity, a typical silica profile, tendency to amorphous structure, low surface area and presence of micropores.

In the adsorption assays performed, in general, the increase of the amount of adsorbent favored the removal of Cr(VI). A higher removal tendency at low pH values was verified for both adsorbents, where best results are obtained at pH 1.0, presenting 90.9% and 97.7% for RHA and RHAH⁺, respectively, in 5 mg L^{-1} of chromium concentration and about 30 minutes of interaction time. At pH 5.0 and 7.0, only the RHAH⁺ showed significant removal values, corresponding to 77.1% and 73.5% respectively, in about 4 hours. The increase in the initial Cr(VI) concentration (from 5 mg L^{-1} to 45 mg L^{-1}) showed the need for longer interaction time between adsorbent-adsorbate to establish equilibrium. A significant higher performance was obtained for the adsorbent chemically treated (RHAH⁺).


Adsorption data were examined via Langmuir and Freundlich isotherms. Although both are efficient to describe the Cr(VI) adsorption process, Freundlich isotherm presented higher R^2_{adj} for RHAH⁺ as adsorbent, since it characterizes better adsorption into heterogeneous surfaces. The data evaluated in this work showed that adsorption of Cr(VI) can be better described by the pseudo-second order kinetic model demonstrating the chemical adsorption that occurs between the adsorbent and adsorbate.

The use of an abundant and low-cost adsorbent, parboiled-rice husk ash, for removing Cr(VI), is a promising alternative for application in effluent treatment. Notwithstanding, further studies are still needed to evaluate the technical and economic feasibility of applying the technology to large wastewater treatment plants.

Acknowledgments

The authors acknowledge the kind support of the Cooperja Agroindustrial Cooperative, Center for Microscopy and Microanalysis (UFRGS), the X-ray Laboratory of the Institute of Physics (UFRGS) and the Multi-User Thermal Analysis Laboratory (UFRGS).

ORCID


Vanessa Schwarztzhaupt Gamboa  <http://orcid.org/0000-0002-9063-2188>

Edilson Valmir Benvenutti  <http://orcid.org/0000-0002-7889-3625>

Éder Júlio Kinast  <http://orcid.org/0000-0001-5822-489X>

Marçal Pires  <http://orcid.org/0000-0003-2247-105X>

Fabiano Perin Gasparin  <http://orcid.org/0000-0001-9422-6948>

Lúcia Allebrandt da Silva Ries  <http://orcid.org/0000-0002-1586-0041>

References

- Agrafioti E, Kalderis D, Diamadopoulou E. 2014. Arsenic and chromium removal from water using biochars derived from rice husk, organic solid wastes and sewage sludge. *J Environ Manage.* 133:309–314. doi:10.1016/j.jenvman.2013.12.007
- Aguiar MRMPd, Novaes AC, Guarino AWS. 2002. Remoção de metais pesados de efluentes industriais por aluminossilicatos. *Quím Nova.* 25(6b):1145–1154. doi:10.1590/S0100-40422002000700015
- Ahmaruzzaman M, Gupta VK. 2011. Rice husk and its ash as low-cost adsorbents in water and wastewater treatment. *Ind Eng Chem Res.* 50(24):13589–13613. doi:10.1021/ie201477c
- Ahmed I, Attar SJ, Parande MG. 2012. Removal of hexavalent chromium (Cr (VI)) from industrial wastewater by using biomass adsorbent (Rice Husk Carbone). *Int J Adv Eng Res.* I(II):92–94.
- Altun T, Kar Y. 2016. Removal of Cr(VI) from aqueous solution by pyrolytic charcoals. *Xinxing Tan Cailiao/New Carbon Mater.* 31(5):501–509. doi:10.1016/S1872-5805(16)60028-8
- American Public Health Association. 1995. *Standard Methods for the Examination of Water and Wastewater.* 19th ed. New York: American Public Health Association.
- Attari M, Bukhari SS, Kazemian H, Rohani S. 2017. A low-cost adsorbent from coal fly ash for mercury removal from industrial wastewater. *J Environ Chem Eng.* 5(1): 391–399. doi:10.1016/j.jece.2016.12.014
- Babel S, Kurniawan TA. 2004. Cr(VI) removal from synthetic wastewater using coconut shell charcoal and commercial activated carbon modified with oxidizing agents and/or chitosan. *Chemosphere.* 54(7):951–967. doi:10.1016/j.chemosphere.2003.10.001
- Bielicka A, Bojanowska I, Wiśniewski A. 2005. Two faces of chromium - Pollutant and bioelement. *Polish J Environ Stud.* 14:5–10.
- Burakov AE, Galunin EV, Burakova IV, Kucherova AE, Agarwal S, Tkachev AG, Gupta VK. 2018. Adsorption of heavy metals on conventional and nanostructured materials for wastewater treatment purposes: a review. *Ecotoxicol Environ Saf.* 148:702–712. doi:10.1016/j.ecoenv.2017.11.034
- CONAMA. 2011. Resolução N° 430, de 13 De Maio De 2011.
- Costa TMH, Gallas MR, Benvenutti EV, Da Jornada JAH. 1997. Infrared and thermogravimetric study of high pressure consolidation in alkoxide silica gel powders. *J Non-Cryst Solids.* 220(2–3):195–201. doi:10.1016/S0022-3093(97)00236-6
- da Silva Ries LA, Silveira JHd. 2019. Remoção de Cr(VI) por adsorção empregando carvão ativado comercial e carvão vegetal produzido a partir da casca de arroz. *BJD.* 5(6):6477–6494. doi:10.34117/bjdv5n6-148
- Dehghani MH, Sanaei D, Ali I, Bhatnagar A. 2016. Removal of chromium(VI) from aqueous solution using treated waste newspaper as a low-cost adsorbent: kinetic modeling and isotherm studies. *J Mol Liq.* 215:671–679. doi:10.1016/j.molliq.2015.12.057
- Della VP, Hotza D, Junkes JA, De Oliveira APN. 2006. Estudo comparativo entre sílica obtida por lixívia ácida da casca de arroz e sílica obtida por tratamento térmico da cinza de casca de arroz. *Quim Nova.* 29:1175–1179. doi:10.1590/s0100-40422006000600005
- Ding D, Ma X, Shi W, Lei Z, Zhang Z. 2016. Insights into mechanisms of hexavalent chromium removal from aqueous solution by using rice husk pretreated using hydrothermal carbonization technology. *RSC Adv.* 6(78): 74675–74682. doi:10.1039/C6RA17707G

- Dotto GL, McKay G. 2020. Current scenario and challenges in adsorption for water treatment. *J Environ Chem Eng.* 8(4):103988. doi:10.1016/j.jece.2020.103988
- El Halal SLM, Colussi R, Deon VG, Pinto VZ, Villanova FA, Carreño NLV, Dias ARG, Zavareze EDR. 2015. Films based on oxidized starch and cellulose from barley. *Carbohydr Polym.* 133:644–653. doi:10.1016/j.carbpol.2015.07.024
- Enniya I, Rghioui L, Jourani A. 2018. Adsorption of hexavalent chromium in aqueous solution on activated carbon prepared from apple peels. *Sustain Chem Pharm.* 7:9–16. doi:10.1016/j.scp.2017.11.003
- Fernandes IJ, Calheiro D, Santos ECAd, Moraes CAM, Rocha TLAdC, Kieling AG, Brehm FA. 2018. Tratamento de Cinza de Casca de Arroz por Lixiviação Ácida, in: *ABM Proceedings*. Editora Blucher, São Paulo, pp. 2209–2216. doi:10.5151/1516-392x-27067.
- Fidalgo A, Ilharco LM. 2001. The defect structure of sol-gel-derived silica/polytetrahydrofuran hybrid films by FTIR. *J Non-Cryst Solids.* 283(1–3):144–154. doi:10.1016/S0022-3093(01)00418-5
- Foletto EL, Hoffmann R, Hoffmann RS, Portugal UL, Jahn SL. 2005. Aplicabilidade das cinzas da casca de arroz. *Quím Nova.* 28(6):1055–1060. doi:10.1590/S0100-40422005000600021
- Food and Agriculture Organization. 2018. Food and agriculture organization of the united nations - Production of rice paddy [WWW Document]. <http://www.fao.org/faostat/en/#data/QC/visualize>. Accessed 2018 July 30.
- Georgieva VG, Tavlieva MP, Genieva SD, Vlaev LT. 2015. Adsorption kinetics of Cr(VI) ions from aqueous solutions onto black rice husk ash. *J Mol Liq.* 208:219–226. doi:10.1016/j.molliq.2015.04.047
- Ghosh R. 2013. A review study on precipitated silica and activated carbon from rice husk. *J Chem Eng Process Technol.* 4(4):1–7. doi:10.4172/2157-7048.1000156.
- Gregg S, Sing K. 1982. Adsorption, surface area and porosity, 2nd ed. London: Academic Press.
- Hamadi NK, Chen XD, Farid MM, Lu MGQ. 2001. Adsorption kinetics for the removal of chromium(VI) from aqueous solution by adsorbents derived from used tyres and sawdust. *Chem Eng J.* 84(2):95–105. doi:10.1016/S1385-8947(01)00194-2
- Ho YS, McKay G. 2000. The kinetics of sorption of divalent metal ions onto sphagnum moss peat. *Water Res.* 34(3): 735–742. doi:10.1016/S0043-1354(99)00232-8
- Kannan N, Sundaram MM. 2001. Kinetics and mechanism of removal of methylene blue by adsorption on various carbons - A comparative study. *Dye Pigment.* 51(1): 25–40. doi:10.1016/S0143-7208(01)00056-0
- Karthikeyan T, Rajgopal S, Miranda LR. 2005. Chromium(VI) adsorption from aqueous solution by Hevea Brasiliensis sawdust activated carbon. *J Hazard Mater.* 124(1–3):192–199. doi:10.1016/j.jhazmat.2005.05.003
- Khandaker S, Kuba T, Kamida S, Uchikawa Y. 2017. Adsorption of cesium from aqueous solution by raw and concentrated nitric acid-modified bamboo charcoal. *J Environ Chem Eng.* 5(2):1456–1464. doi:10.1016/j.jece.2017.02.014
- Kieling AG, Mendel T, Caetano MO. 2019. Efficiency of rice husk ash to adsorb chromium(VI) using the Allium cepa toxicity test. *Environ Sci Pollut Res Int.* 26(28): 28491–28499. doi:10.1007/s11356-018-3722-3
- Lin C, Luo W, Luo T, Zhou Q, Li H, Jing L. 2018. A study on adsorption of Cr (VI) by modified rice straw: characteristics, performances and mechanism. *J Clean Prod.* 196:626–634. doi:10.1016/j.jclepro.2018.05.279
- Liu SX, Chen X, Chen XY, Liu ZF, Wang HL. 2007. Activated carbon with excellent chromium(VI) adsorption performance prepared by acid-base surface modification. *J Hazard Mater.* 141(1):315–319. doi:10.1016/j.jhazmat.2006.07.006
- Lopes MFdL, Lopes AdM. 2008. Aspectos Qualitativos e Nutricionais do Arroz. ENCONTRO TÉCNICO “TECNOLOGIAS PARA A PRODUÇÃO ARROZ NO SUDESTE PARAENSE”, 1., 2008, São Geraldo do Araguaia. An. Artig. e palestras. Belém, PA: Embrapa Amaz. Orient. 2008. p. 105–120.
- Martini S, Afrose S, Ahmad Roni K. 2020. Modified eucalyptus bark as a sorbent for simultaneous removal of COD, oil, and Cr(III) from industrial wastewater. *Alex Eng J.* 59(3):1637–1648. doi:10.1016/j.aej.2020.04.010
- Mitra T, Bar N, Das SK. 2019. Rice husk: green adsorbent for Pb(II) and Cr(VI) removal from aqueous solution—column study and GA–NN modeling. *SN Appl Sci.* 1(5): 1–15. doi:10.1007/s42452-019-0513-5
- Moayedi H, Aghel B, Abdullahi MM, Nguyen H, Safuan A Rashid A. 2019. Applications of rice husk ash as green and sustainable biomass. *J Clean Prod.* 237:117851. doi:10.1016/j.jclepro.2019.117851
- Mor S, Chhoden K, Ravindra K. 2016. Application of agro-waste rice husk ash for the removal of phosphate from the wastewater. *J Clean Prod.* 129:673–680. doi:10.1016/j.jclepro.2016.03.088
- Nascimento Rfd, Lima ACAd, Vidal CB, Melo DdQ, Raulino GSC. 2014. Adsorção: Aspectos teóricos e aplicações ambientais, 1st ed. Fortaleza: Imprensa Universitária.
- Paraginski RT, Ziegler V, Talhamento A, Elias MC, Oliveira Md. 2014. Propriedades tecnológicas e de cocção em grãos de arroz condicionados em diferentes temperaturas antes da parboilização. *Braz J Food Technol.* 17(2): 146–153. doi:10.1590/bjft.2014.021
- Ponou J, Kim J, Wang LP, Dodbiba G, Fujita T. 2011. Sorption of Cr(VI) anions in aqueous solution using carbonized or dried pineapple leaves. *Chem Eng J.* 172(2–3): 906–913. doi:10.1016/j.cej.2011.06.081
- Rahaman MA, Akther N, Patwary MAM. 2015. Comparative adsorption study on rice husk and rice husk ash by using amaranthus gangeticus pigments as dye. *Eur Sci J.* 11:254–265.
- Raposo F, De La Rubia MA, Borja R. 2009. Methylene blue number as useful indicator to evaluate the adsorptive

- capacity of granular activated carbon in batch mode: influence of adsorbate/adsorbent mass ratio and particle size. *J Hazard Mater.* 165(1–3):291–299. doi:10.1016/j.jhazmat.2008.09.106
- Roisnel T, Rodríguez-Carvajal J. 2001. WinPLOTR: a windows tool for powder diffraction pattern analysis. *MSF.* 378–381:118–123. doi:10.4028/www.scientific.net/MSF.378-381.118
- Salas J, Gómez G, Veras J. 1986. Hormigones con ceniza de cascara de arroz (R.H.A.). *Inf Constr.* 38(385):31–41. doi:10.3989/ic.1986.v38.i385.1692
- Sharma DC, Forster CF. 1994. A preliminary examination into the adsorption of hexavalent chromium using low-cost adsorbents. *Bioresour Technol.* 47(3):257–264. doi:10.1016/0960-8524(94)90189-9
- Singha B, Das SK. 2011. Biosorption of Cr(VI) ions from aqueous solutions: kinetics, equilibrium, thermodynamics and desorption studies. *Colloids Surf B Biointerfaces.* 84(1):221–232. doi:10.1016/j.colsurfb.2011.01.004
- Singh SR, Singh AP. 2012. Treatment of water containing chromium (VI) using rice husk carbon as a new low cost adsorbent. *Int J Environ Res.* 6:917–924. doi:10.22059/ijer.2012.562.
- Singh V, Singh J, Mishra V. 2021. Development of a cost-effective, recyclable and viable metal ion doped adsorbent for simultaneous adsorption and reduction of toxic Cr (VI) ions. *J Environ Chem Eng.* 9(2):105124. doi:10.1016/j.jece.2021.105124
- Song M, Wei Y, Cai S, Yu L, Zhong Z, Jin B. 2018. Study on adsorption properties and mechanism of Pb²⁺ with different carbon based adsorbents. *Sci Total Environ.* 618:1416–1422. doi:10.1016/j.scitotenv.2017.09.268
- Srivastava V, Weng CH, Sharma YC. 2013. Application of a thermally modified agrowaste material for an economically viable removal of Cr(VI) from aqueous solutions. *J Hazard Toxic Radioact Waste.* 17(2):125–133. doi:10.1061/(ASCE)HZ.2153-5515.0000168
- Wan Ngah WS, Hanafiah MAKM. 2008. Removal of heavy metal ions from wastewater by chemically modified plant wastes as adsorbents: a review. *Bioresour Technol.* 99(10):3935–3948. doi:10.1016/j.biortech.2007.06.011
- Weidinger A, Hermans PH. 1961. On the determination of the crystalline fraction of isotactic polypropylene from x-ray diffraction. *Makromol Chem.* 50(1):98–115. doi:10.1002/macp.1961.020500107
- Wright AF, Leadbetter AJ. 1975. The structures of the β -cristobalite phases of SiO₂ and A₁PO₄. *Philos Mag.* 31(6):1391–1401. doi:10.1080/00318087508228690
- Wu Y, Ming Z, Yang S, Fan Y, Fang P, Sha H, Cha L. 2017. Adsorption of hexavalent chromium onto Bamboo Charcoal grafted by Cu²⁺-N-aminopropylsilane complexes: optimization, kinetic, and isotherm studies. *J Ind Eng Chem.* 46:222–233. doi:10.1016/j.jiec.2016.10.034
- Xiong L, Sekiya EH, Sujaridworakun P, Wada S, Saito K. 2009. Burning temperature dependence of rice husk ashes in structure and property. *J Met Mater Miner.* 19:95–99.
- Yi Y, Tu G, Zhao D, Tsang PE, Fang Z. 2019. Biomass waste components significantly influence the removal of Cr(VI) using magnetic biochar derived from four types of feedstocks and steel pickling waste liquor. *Chem Eng J.* 360:212–220. doi:10.1016/j.cej.2018.11.205
- Zeljko S, Penavin-Skundric J, Jelic D, Sladojevic S, Vasiljevic L. 2015. Interaction of hexavalent chromium and BSCF perovskite in water solutions. *Zas Mat.* 56(3):340–344. doi:10.5937/ZasMat1503340Z
- Zhao N, Wei N, Li J, Qiao Z, Cui J, He F. 2005. Surface properties of chemically modified activated carbons for adsorption rate of Cr (VI). *Chem Eng J.* 115(1–2):133–138. doi:10.1016/j.cej.2005.09.017